Experimental and theoretical investigations on the keto–enol tautomerism of 4-substituted 3-[1-methylpyrrol-2-yl)methyl]-4,5-dihydro-1H-1,2,4-triazol-5-one derivatives

ARTICLE *in* JOURNAL OF MOLECULAR STRUCTURE · MAY 2011

Impact Factor: 1.6 · DOI: 10.1016/j.molstruc.2011.03.041

5 AUTHORS, INCLUDING:

Monika Pitucha
Medical University of Lublin
42 PUBLICATIONS **204** CITATIONS
SEE PROFILE

Waldemar Wysocki
Siedlce University of Natural Sciences and…
37 PUBLICATIONS **65** CITATIONS
SEE PROFILE

Agnieszka Kaczor
Medical University of Lublin
53 PUBLICATIONS **232** CITATIONS
SEE PROFILE

Dariusz Matosiuk
Medical University of Lublin
90 PUBLICATIONS **644** CITATIONS
SEE PROFILE

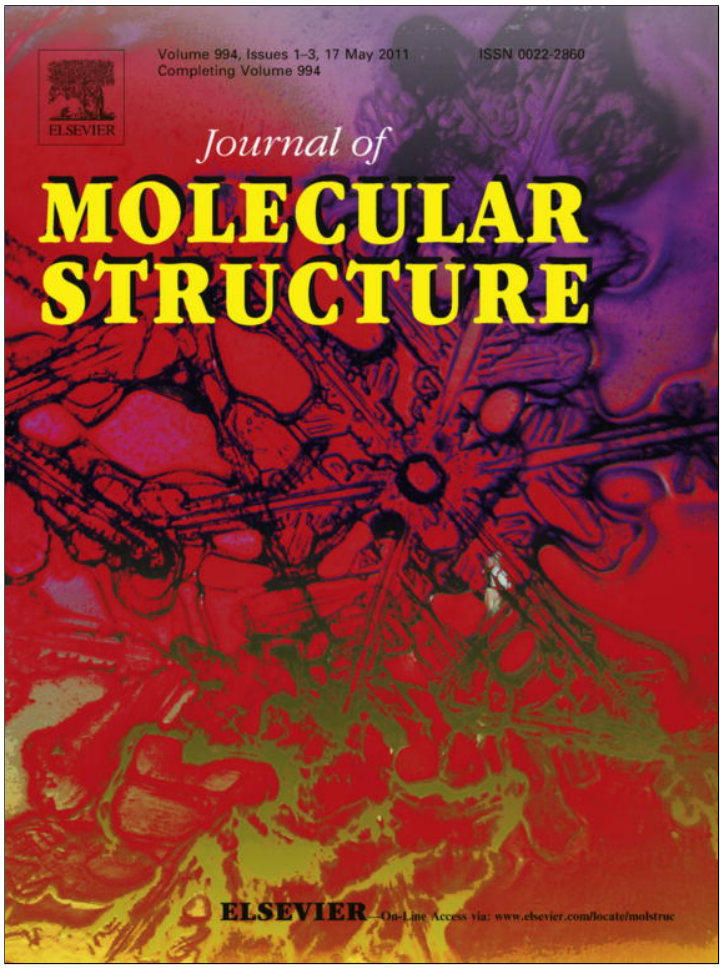

Journal of Molecular Structure 994 (2011) 313–320

Contents lists available at ScienceDirect

Journal of Molecular Structure

journal homepage: www.elsevier.com/locate/molstruc

Experimental and theoretical investigations on the keto–enol tautomerism of 4-substituted 3-[1-methylpyrrol-2-yl)methyl]-4,5-dihydro-1*H*-1,2,4-triazol-5-one derivatives

Monika Pitucha [a,*], Zbigniew Karczmarzyk [b], Waldemar Wysocki [b], Agnieszka A. Kaczor [c], Dariusz Matosiuk [c]

[a] Department of Organic Chemistry, Faculty of Pharmacy, Medical University of Lublin, 6 Staszica St., 20081 Lublin, Poland
[b] Department of Chemistry, University of Podlasie, 3 Maja 54 St., 08110 Siedlce, Poland
[c] Department of Synthesis and Chemical Technology of Pharmaceutical Substances, Faculty of Pharmacy, Medical University of Lublin, 6 Staszica St., 20081 Lublin, Poland

ARTICLE INFO

Article history:
Received 15 December 2010
Received in revised form 16 March 2011
Accepted 16 March 2011
Available online 25 March 2011

Keywords:
Keto–enol tautomerism
X-ray structure determination
Quantum chemical calculation
1,2,4-Triazoles

ABSTRACT

Keto–enol tautomerism is a key phenomenon which determines the pharmacological activity of compounds possessing the carbonyl group. In the present study we use X-ray analysis, IR spectroscopy as well as quantum chemical calculation to address the keto–enol tautomerism of 4-substituted 3-[1-methylpyrrol-2-yl)methyl]-4,5-dihydro-1*H*-1,2,4-triazol-5-one derivatives with antimicrobial activity. In the gas phase and in the crystalline state all the investigated molecules exist in the keto form while in the chloroform solution a small amount of the enol form in the equilibrium with the keto form is observed. The results of the calculations are in good agreement with experimental data obtained from X-ray analysis and IR spectroscopy in KBr but do not confirm the shift of the tautomeric equilibrium into the enol form in a chloroform solution.

1. Introduction

Keto–enol tautomerism plays a crucial role in compounds possessing the carbonyl group. Investigations on the tautomeric equilibrium in carbonyl compounds are very important to rationalize their biological activity [1–7] and to understand biochemical processes in which they take part. The best known examples of keto–enol tautomerism in nature are nitrogenous bases in which shifting the equilibrium to the keto form makes it possible to form hydrogen bonds to maintain the double-strand structure of DNA. Besides nucleic acids, many pharmacologically active compounds have their activity determined by the relative greater stability of one tautomer. Examples of such compounds are phosphorohydrazine derivatives of coumarin and chromone which have antibacterial and antitumor activity conditioned by the keto–enol tautomerism [2]. Some compounds exhibiting keto–enol tautomerism which affects their opioid and serotonin receptor activity have also been obtained by our research group [3–6]. Furthermore, the greater stability of a keto or an enol form of a compound may be crucial for the interaction with the target binding site. As it has been recently shown by Temperini et al. [7], the binding site itself may preferentially stabilize one of the tautomers as in the case of the enol form of chlorthalidone binding to the active site of carbonic anhydrase.

An important class of compounds exhibiting keto–enol tautomerism are carbonyl derivatives of 1,2,4-triazole. The 1,2,4-triazole system is present in a great number of compounds characterized by different biological activities, such as: analgesic [8,9] antibacterial [10–13], fungicidal [14], antinflammatory [15–17], antiviral [18,19] and anti-cancer [20–22] properties. Based on these facts, many 1,2,4-triazol-5-one derivatives have been synthesized in our laboratory and their biological activities have been investigated [23–27]. These compounds were mainly synthesized by the cyclization of their semicarbazide derivatives in alkaline media. Searching for new biologically active 1,2,4-triazole derivatives, we obtained, among others, 4-substituted-3-[(1-methylpyrrol-2-yl)methyl]-4,5-dihydro-1*H*-1,2,4-triazol-5-one derivatives **1–6** (Fig. 1). These compounds were screened for their antimicrobial [26] and central nervous system activities [27]. In order to rationalize the biological activity of the investigated compounds, we decided to study their keto–enol tautomerism as it had been demonstrated that the relative stability of the keto and the enol form may affect pharmacological activity in similar systems [6]. The knowledge about relative stability of keto and enol tautomers is an essential condition to perform structure–activity studies (SAR) as well as molecular docking because the presence of a hydroxyl or a carbonyl group may dramatically change the interactions of compounds **1–6** with bacterial enzymes. In general,

* Corresponding author. Tel.: +48 815357373.
E-mail address: monika.pitucha@umlub.pl (M. Pitucha).

0022-2860/$ - see front matter © 2011 Elsevier B.V. All rights reserved.
doi:10.1016/j.molstruc.2011.03.041

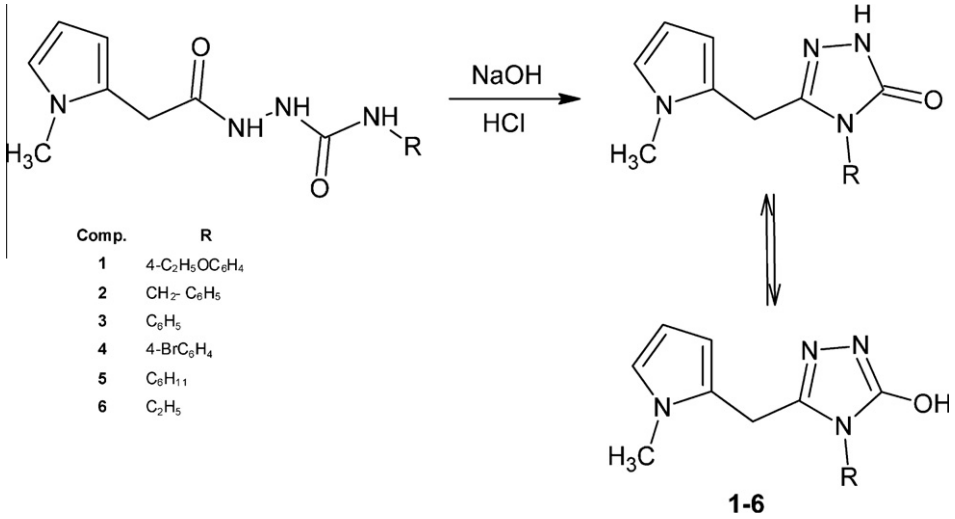

Fig. 1. The synthesis and keto–enol tautomerism of the investigated compounds.

application of any computer-assisted drug design methods to a series of compounds for which keto–enol tautomerism is possible, should be preceded by determination which tautomer is energetically privileged.

It is well established that quantum chemical calculations are very useful in the determination of the most stable structure of tautomers and the estimation of tautomeric equilibrium constants [28,29], in particular when the results of the calculations are confirmed by experimental data. Many such studies have been reported for different classes of compounds, e.g. pyrazolones [30], betaketonitriles [31], cyclohexanediones [32,33]. On the other hand, 1,2,4-triazol-5-one system, bearing different substituents, has been a subject of extensive experimental and computational studies which were aimed to determine structural and spectral properties of respective derivatives [34–40].

In the light of above, in this study, we report the analysis of the tautomeric equilibrium between the keto and enol forms for the 1,2,4-triazole-5-one system in **1–6** using quantum chemical calculations in the gas phase and in solutions, supported by IR spectroscopy and X-ray analysis in the crystalline state. We show that in the gas phase and in the crystalline state all molecules exist in the keto form while in the chloroform solution a small amount of the enol form in the equilibrium with the keto form is observed.

2. Experimental

2.1. Synthesis

4-substituted 3-[(1-methylpyrrol-2-yl)methyl]-4,5-dihydro-1*H*-1,2,4-triazol-5-one derivatives **1–6** were synthesized by the intramolecular dehydrative cyclization of the respective 4-substituted-1-[(1-methylpyrrol-2-yl)acetyl]semicarbazides (obtained from the reaction of 1-methylpyrrol-2-yl-acetic acid hydrazide with the appropriate isocyanate) according to the procedure earlier reported, Fig. 1 [26].

2.2. IR spectra

IR spectra of **1–6** were measured in the solid state (KBr) and in chloroform with a Magna IR-760 Nicolet spectrophotometer. Before IR measurements, chloroform (analytically pure) was dehydrated using $CaCl_2$ and then distilled off with dephlegmator (with no moisture).

2.3. X-ray investigation of *1*

Light brown prismatic crystals of **1** suitable for X-ray diffraction analysis were grown by slow evaporation of an ethanol solution. X-ray data were collected on the Bruker SMART APEX CCD diffractometer at room temperature; crystal sizes: 0.50 × 0.25 × 0.18 mm, ω scans. The structure was solved by direct methods using SIR92 [41] and refined by full matrix least squares with SHELXL97 [42]. All hydrogen atoms were located from the $\Delta\rho$ map and their coordinates were refined with isotropic displacement parameters taken as 1.5 times those of the respective parent atoms. All crystal and experimental data are listed in Table 1.

Molecular graphics were prepared using ORTEP3 for Windows [45]. PARST [46] and PLATON [47] were used for geometrical

Table 1
Crystal data and structure refinement for **1**.

Empirical formula	$C_{16}H_{18}N_4O_2$
Formula weight	298.34
Crystal system	monoclinic
Space group	$P2_1$
Unit cell parameters	a = 7.6707(15) Å
	b = 7.2466(14) Å
	c = 14.307(3) Å
	β = 103.37(3)°
Volume, V	773.7(3) Å^3
Molecular multiplicity, Z	2
Density (calculated)	1.281 g/cm^3
Radiation	Cu Kα (λ = 1.54178 Å)
Cell parameters from	61 Reflections
θ range for lattice parameters	7.10–39.15°
Absorption coefficient, μ	0.711 mm^{-1}
Absorption correction	Multi-scan [43]
T_{min}/T_{max}	0.8185/0.9323
θ range for data collection	3.17–70.04°
Index ranges h, k, l	−9/9, −7/8, −17/17
No. of measured reflections	8833
No. of independent reflections	2579 (R_{int} = 0.0162)
No. of observed reflection	2541 with $I > 2\sigma(I)$
Refinement	
Refinement method	Full-matrix least-squares on F^2
Final R indices: R, $wR(F^2)$	0.0353, 0.1023
Goodness-of-fit on F^2, S	1.046
Data/restraints/parameters	2579/1/255
Absolute structure parameter	0.0(2) [44]
Extinction coefficient	0.0028(14)
Largest diff. peak and hole	+0.157/−0.139 eÅ^{-3}
$(\Delta/\sigma)_{max}$	0.068

calculations. All calculations were performed using WINGX ver. 1.64.05 package [48]. CCDC-618948 for **1** contains the supplementary crystallographic data for this paper. These data can be obtained free of charge at www.ccdc.cam.ac.uk/conts/retrieving.html (or from the Cambridge Crystallographic Data Centre (CCDC), 12 Union Road, Cambridge CB2 1EZ, UK; fax: +44(0) 1223 336 033; email: deposit@ccdc.cam.ac.uk).

2.4. Theoretical calculations

The molecular structure of **1** in the ground state was optimized with the Hartree–Fock and B3LYP DFT (the variant of DFT method using Becke's three-parameter hybrid functional (B3) [49] with correlation functional such as the one proposed by Lee, Yang, and Parr (LYP) [50]) applying 6-31G(d,p) basis set as included in Gaussian03 [51]. The choice of the computation level, in particular of basis set, was dictated by a compromise between the accuracy of expected results and the resources required. The X-ray structure of **1** was used as the starting conformation for the calculation. In order to identify low energy conformers, five selected degrees of torsional freedom, N2—C3—C6—C7, C3—C6—C7—N8, C5—N4—C21—C22, C23—C24—O27—C28 and C24—O27—C28—C29 were varied from −180° to +180° in steps of 10°, and the respective molecular energy profiles were determined at the molecular mechanics level with the MOE Molecular Operating Environment [52]. To investigate the keto–enole tautomerism of the compound, the population of the tautomers was estimated using non-degenerate Boltzman distribution on the level of 6-31G(d,p)/HF and 6-31G(d,p)/B3LYP. The energy was calculated for isolated molecules (gas phase) and the molecules in chloroform (ε = 4.7113) and water (ε = 78.3553) solutions. Calculations were performed using the Polarizable Continuum Model (PCM) [53]. This method creates a solute cavity via a set of overlapping spheres. Gaussian03 was also used to calculate vibrational frequencies (with 6-31G(d,p)/HF and 6-31G(d,p)/B3LYP methods). The vibrational band assignments were made using the Gauss-View Molecular Visualization program [54,55]. Vibrational frequencies were scaled by 0.8992 [56] for 6-31G(d,p)/HF and by 0.9608 for 6-31G(d,p)/B3LYP [57]. Additionally, alternative scaling factors of IR frequencies were proposed for this group of compounds by taking the average ratio of experimental and computed frequencies, separately for each band and each environment. The following software was also used for visualizing results: Chimera [58], Mercury [59], VegaZZ [60], Yasara Structure [61], PyMol [62] and MOE Molecular Operating Environment [52].

3. Results and discussion

3.1. IR spectra

In order to determine the keto–enol tautomerism of the investigated compounds **1–6**, first the IR spectra were recorded in solid state (KBr) and in chloroform solution. Then, the IR frequencies were calculated with Gaussian03 applying the Hartree–Fock and B3LYP DFT methods and 6-31G(d,p) basis set. All experimental spectra for **1–6** exhibit characteristic bands for the C=O and N—H groups in KBr and additional weak and broad bands for the O—H group in chloroform solution. The characteristic bands (experimental and computed, both raw and scaled) involved in keto–enol tautomerism of analyzed compounds are collected in Table 2.

The calculated "raw" HF and DFT frequencies are usually significantly overestimated in comparison to the experimental values because of the lack of electron correlation, an insufficient basis set and anharmonicity [63]. Thus, we used the scaling factors

Table 2
Experimental and computed IR frequencies involved in the keto–enol tautomerism of compounds **1–6**.

Compound	IR	N—H (cm^{-1})						C=O (cm^{-1})						O—H (cm^{-1})					
R		Exp.	HF			DFT		Exp.	HF			DFT		Exp.	HF			DFT	
			Raw	Scaled[a]	Scaled[b]	Raw	Scaled[a]	Scaled[b]		Raw	Scaled[a]	Scaled[b]	Raw	Scaled[a]	Scaled[b]		Raw	Scaled[a]	Scaled[b]	Raw	Scaled[a]	Scaled[b]
1	KBr	3383	3965	3565	3378	3699	3554	3370	1707	1995	1794	1708	1848	1776	1709	NA	NA	NA	NA	NA	3205
	$CHCl_3$	3469	3854	3466	3427	3618	3476	3437	1712	1946	1750	1713	1813	1742	1713	3190	4113	3698	3223	3734	3588	NA
2	KBr	3393	3958	3559	3372	3701	3556	3372	1709	1975	1776	1691	1824	1752	1687	NA	NA	NA	NA	NA	NA	3171
	$CHCl_3$	3371	3869	3479	3440	3615	3473	3435	1707	1927	1733	1696	1795	1725	1696	3190	4037	3630	3163	3694	3549	NA
3	KBr	3380	3955	3556	3369	3703	3558	3373	1705	1996	1795	1709	1849	1777	1710	NA	NA	NA	NA	NA	NA	3216
	$CHCl_3$	3468	3851	3463	3424	3606	3465	3426	1708	1947	1751	1714	1811	1740	1711	3194	4105	3691	3217	3747	3600	NA
4	KBr	3381	3956	3557	3370	3697	3552	3368	1706	1997	1796	1709	1849	1777	1710	NA	NA	NA	NA	NA	NA	3226
	$CHCl_3$	3467	3855	3466	3428	3604	3463	3424	1710	1949	1753	1715	1818	1747	1717	3200	4110	3696	3221	3758	3611	NA
5	KBr	3365	3965	3565	3378	3708	3563	3378	1691	1968	1770	1685	1820	1749	1683	NA	NA	NA	NA	NA	NA	3154
	$CHCl_3$	3470	3856	3467	3429	3606	3465	3426	1697	1927	1733	1696	1795	1725	1696	3166	4031	3625	3159	3674	3530	NA
6	KBr	3337	3958	3559	3372	3709	3564	3379	1679	1981	1781	1696	1837	1765	1699	NA	NA	NA	NA	NA	NA	3166
	$CHCl_3$	3340	3865	3475	3437	3618	3476	3437	1702	1934	1739	1702	1803	1732	1703	3197	4028	3622	3156	3688	3543	3205

NA = not available.
[a] Scaling with scaling factors available in literature.
[b] Scaling with scaling factors calculated separately for each band; see explanation in the text.

available in literature to enhance the computation results. Vibrational frequencies were scaled by 0.8992 [56] for 6-31G(d,p)/HF and by 0.9608 [57] for 6-31G(d,p)/B3LYP. This led to the accordance of experimental and computed frequencies for the spectra recorded in chloroform (with the exception of frequencies for the hydroxylic group) but not in the solid state. Therefore it was decided to check what scaling factors would be suitable for this group of compounds by calculating the average ratio of experimental and computed frequency for each method in each environment separately. The obtained scaling factors were 0.8540 and 0.9179 for the spectra in KBr, for HF and DFT method, respectively and varied significantly from the scaling factors available in literature. The same procedure applied to the spectra recorded in chloroform resulted in the factors 0.8510 and 0.9177 for HF and DFT methods, respectively. To improve further the calculated frequencies, the scaling factors were calculated for each band separately which is a common practice [64,65], with the scaling factors reported up to now the range from about 0.78 to slightly above 1. The summary on the applied scaling factors is given in Table 3. The final scaling was performed with the separate scaling factors for each band. Thus, restricting them to the analyzed functional groups, the proposed scaling factors may lead to an enhancement of the calculated IR frequencies for the similar compounds [65]. As a result of this part of the study it may be concluded that the keto form is the one existing in the solid state. In chloroform solution besides the keto form a small amount of an enol form is observed and equilibrium between both keto and enol forms is reached. Additionally, ^{1}H NMR spectra in chloroform were recorded for the investigated compounds but they did not exhibit the signal of the enol from.

Table 3
The applied scaling factors.

Scaling	KBr		Chloroform	
	HF/6-31G(d,p)	B3LYP/6-31G(d,p)	HF/6-31G(d,p)	B3LYP/6-31G(d,p)
Refs. [45,46]	0.8992	0.9608	0.8992	0.9608
Average for all the bands	0.8540av	0.9179	0.8510	0.9177
Separate for each band				
N—H	0.8519	0.9110	0.8892	0.9501
C=O	0.8560	0.9248	0.8801	0.9447
O—H	NA	NA	0.7836	0.8584

NA = not available.

3.2. X-ray and computed structure of **1**

In order to identify the molecular structure and the tautomeric form in the solid state of the investigated compound, X-ray structure analysis followed by quantum chemical calculations for **1** were performed. The selected geometrical parameters for the crystal structure of **1** are given in Table 4. A view of the molecule with numbering of the atoms is shown in Fig. 2 and the packing of molecules in the crystal network is presented in Fig. 3.

The difference electron density map for molecule **1** revealed the position of the H atom in the vicinity of the N1 atom. Additionally, the C5—O5 bond length of 1.2323(17) Å is typical for the bond length in a carbonyl group [66]. These two facts explicitly indicate that the keto tautomeric form of **1** is the only one existing in the crystalline state. Bond lengths and angles in the triazolone and pyrrole ring systems do not differ significantly from those reported for other related structures [67,68]. The 1,2,4-triazole (*A*), pyrrole (*B*) and phenyl (*C*) rings are planar to within 0.006(1), 0.007(3) and 0.024(1) Å and the dihedral angles between the planes of these rings are $A/B = 63.14(7)^\circ$, $A/C = 55.55(5)^\circ$, $B/C = 62.36(7)^\circ$. The 3-[(1-methylpyrrole-2-yl)methyl] substituent adopts gauche–gauche conformation with torsion angles N2—C3—C6—C7 and C3—C6—C7—N8 of $-98.5(2)^\circ$ and $85.2(2)^\circ$, respectively. The ethoxy group is almost co-planar with the phenyl ring and it adopts trans–trans conformation with the torsion angles C23—C24—O27—C28 = $174.35(16)^\circ$ and C24—O27—C28—C29 = $-176.90(19)^\circ$. The conformation of the molecule observed in the crystal of **1** is forced by steric repulsion between two large substituents in the adjacent 3 and 4 positions of the triazole ring. In the crystal structure the molecules related by the 21 symmetry axis are joined in molecular chains parallel to the Y crystallographic axis by N1—H11···O5 ($1-x$, $-1/2+y$, $-z$) hydrogen bond: N1—H11 = 0.95(3) Å, H11···O5 = 1.88(3) Å, N1···O5=2.810(2) Å, N—H11···O5=166(2)°. Additionally, the intermolecular C—H···π contact involving the pyrrole ring is observed with C28···Cg1=3.575(3)Å, H282···Cg1 = 2.87(4) Å and C28—H282···Cg1 = 125(2)°; Cg1 is the centroid of the pyrrole (x, $1+y$, z) ring.

Table 4
Experimental and computed geometrical parameters of **1**.

Parameter	Experimental	Computed, 6-31G(d,p)	
		HF	DFT
Bond			
O5—C5	1.2323(17)	1.197	1.218
N1—C5	1.346(2)	1.352	1.375
N1—N2	1.3875(17)	1.370	1.379
N2—C3	1.292(2)	1.270	1.303
N4—C3	1.3842(18)	1.381	1.386
N4—C5	1.3845(19)	1.387	1.416
N4—C21	1.432(2)	1.426	1.427
N8—C7	1.372(3)	1.370	1.384
N8—C9	1.381(3)	1.363	1.376
N8—C12	1.455(3)	1.449	1.455
C3—C6	1.4986(19)	1.502	1.505
C6—C7	1.492(2)	1.506	1.506
C7—C11	1.378(3)	1.362	1.383
C9—C10	1.346(5)	1.358	1.377
C10—C11	1.394(4)	1.421	1.421
Bond angle			
C5—N1—N2	112.37(13)	113.26	114.21
C3—N2—N1	104.90(13)	105.10	104.47
C3—N4—C5	107.44(12)	107.62	108.07
C3—N4—C21	128.37(12)	128.59	128.63
C5—N4—C21	123.90(11)	123.67	123.28
C9—N8—C7	106.9(2)	108.56	108.83
C9—N8—C12	126.5(2)	124.18	124.56
C7—N8—C12	126.36(18)	126.78	126.27
N2—C3—N4	111.29(12)	111.59	111.74
N2—C3—C6	123.19(14)	123.69	122.97
N4—C3—C6	125.52(15)	124.71	125.20
O5—C5—N1	128.49(15)	129.38	129.99
O5—C5—N4	127.52(15)	128.20	128.51
N1—C5—N4	103.99(11)	102.41	101.51
C7—C6—C3	115.28(13)	114.53	114.11
C11—C7—N8	108.48(18)	108.20	107.74
C11—C7—C6	129.0(2)	128.79	129.49
N8—C7—C6	122.40(17)	123.01	122.76
C10—C9—N8	109.7(3)	109.14	108.69
C9—C10—C11	107.5(2)	106.64	107.01
C7—C11—C10	107.4(3)	107.46	107.73
Torsion angles			
N2—C3—C6—C7	−98.5(2)	−101.43	−103.53
C3—C6—C7—N8	85.2(2)	76.05	75.54
C5—N4—C21—C22	52.12(19)	84.01	61.14
C23—C24—O27—C28	174.35(16)	−178.13	−179.19
C24—O27—C28—C29	−176.90(13)	178.93	179.87

Gaussian03 was used to optimize the geometry of the investigated compound on the level of Hartree–Fock and B3LYP DFT with 6-31G(d,p) basis set. Some selected computed geometrical parameters along with the X-ray analysis parameters are listed in Table 4.

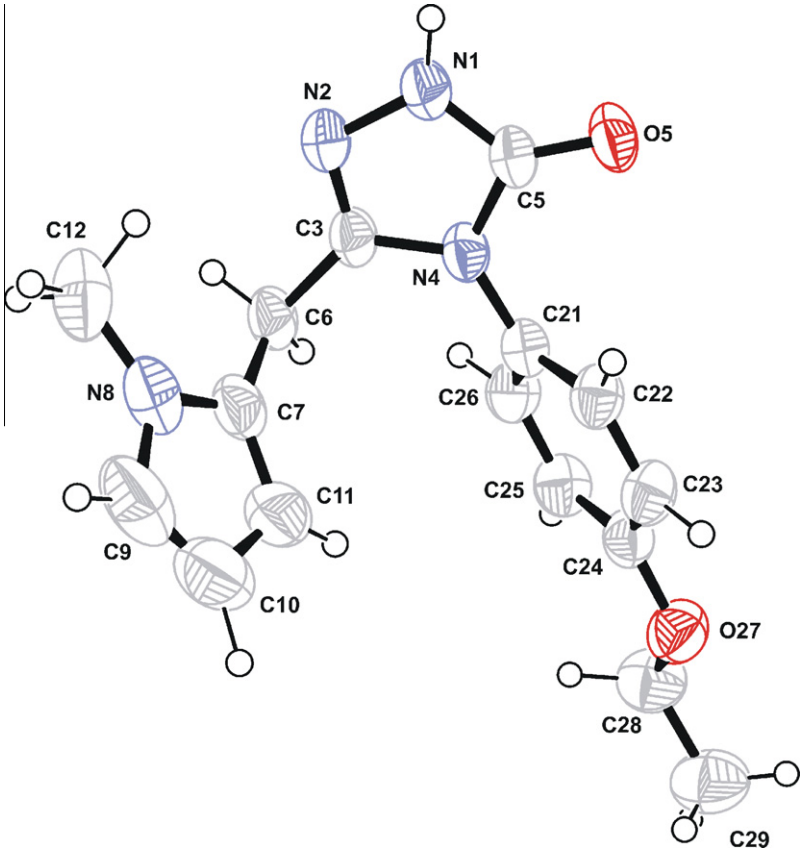

Fig. 2. A view of compound **1** showing the atom-numbering scheme. Displacement ellipsoids for non-H atoms are drawn at the 50% probability level.

The computed structures were aligned with the X-ray structure with root mean square deviation (RMSD, not taking into consideration hydrogen atoms) of 0.4242 Å and 0.2592 Å for HF and B3LYP DFT, respectively (Fig. 4). The good accordance between experimental and computed data is also indicated by correlation coefficients, R^2. These are 0.9896 and 0.9824 for bond lengths and 0.9910 and 0.9865 for bond angles for HF and B3LYP DFT, respectively. The discrepancies between the experimental and computed results may be explained by the fact that the theoretical calculations refer to the gaseous phase whereas the X-ray results refer to the solid state in which the existence of the crystal field along with the intermolecular interactions which have connected the molecules together changes the bond lengths and angles [63]. Although in general DFT-based geometry should be a better approximation of the experimental geometry due to inclusion of electron correlation, in the case of the investigated compound this trend is reversed as indicated by the correlation coefficients given above. The largest difference between experimental and computed bond length was 0.035 Å for the HF method and 0.031 Å for B3LYP DFT whereas the values for bond angles were 2.32° and 2.48°, respectively. Much greater discrepancies are observed in the values of torsion angles which are in the range of 3–30°. Thus, in order to define the preferred position of the methylpyrrol group to the 1,2,4-triazole system, and the ethoxy substituents to the phenyl ring, conformational analysis was performed on the five degrees of conformational freedom: N2—C3—C6—C7, C3—C6—C7—N8, C5—N4—C21—C22, C23—C24—O27—C28 and C24—O27—C28—C29 at the molecular mechanics level with the MOE Molecular Operating Environment [52]. Molecular energy profiles referring to the rotations about the selected torsion angles are depicted in Fig. 5. According to the results the low energy domains for N2—C3—C6—C7 are located at −110° and 30°, while they are located at −180° to −140° and at 75° for the torsion angle C3—C6—C7—N8. Next, the low energy domains for C5—N4—C21—C22 are located at −130° and 45°, while they are located at −180° and 180° for the torsion angles C23—C24—O27—C28 and C24—O27—C28—C29. The results of conformational analysis are in good accordance with the results of the X-ray analysis and the quantum chemical calculations for **1**.

To characterize the structure of **1** in more detail, the Mulliken atomic charges and natural population analysis (NPA) atomic charges for the non-hydrogen atoms of the title compound calculated at HF/6-31G(d,p) and B3LYP/6-31G(d,p) levels were calculated and collected in Table S1 in Supplementary Information. Negative charge is accumulated on heteroatoms (nitrogen and oxygen atoms) whereas the largest positive charge is accumulated on C3 and C5 carbon atoms.

3.3. Theoretical calculations of keto–enol tautomerism

The energy for both the keto and enol tautomers of **1–6** was calculated for isolated molecules (gas phase) and the molecules in chloroform and water solutions. The results of the calculations are presented in Table 5.

It can be seen from Table 5, that the keto form is the one existing in the crystalline state and this form is the most energetically stable in the analyzed solutions. The population of the enol form estimated using non-degenerate Boltzman distribution is less than 0.01% in all considered states. The energy differences between the keto and enol forms change in the relatively narrow range of 8.19–22.30 kcal/mol for all investigated molecules **1–6** and do not depend on the type of substituent in 4 position of 1,2,4-triazole ring and polarity of solvent. The results of the calculations are in good agreement with the experimental data obtained from X-ray

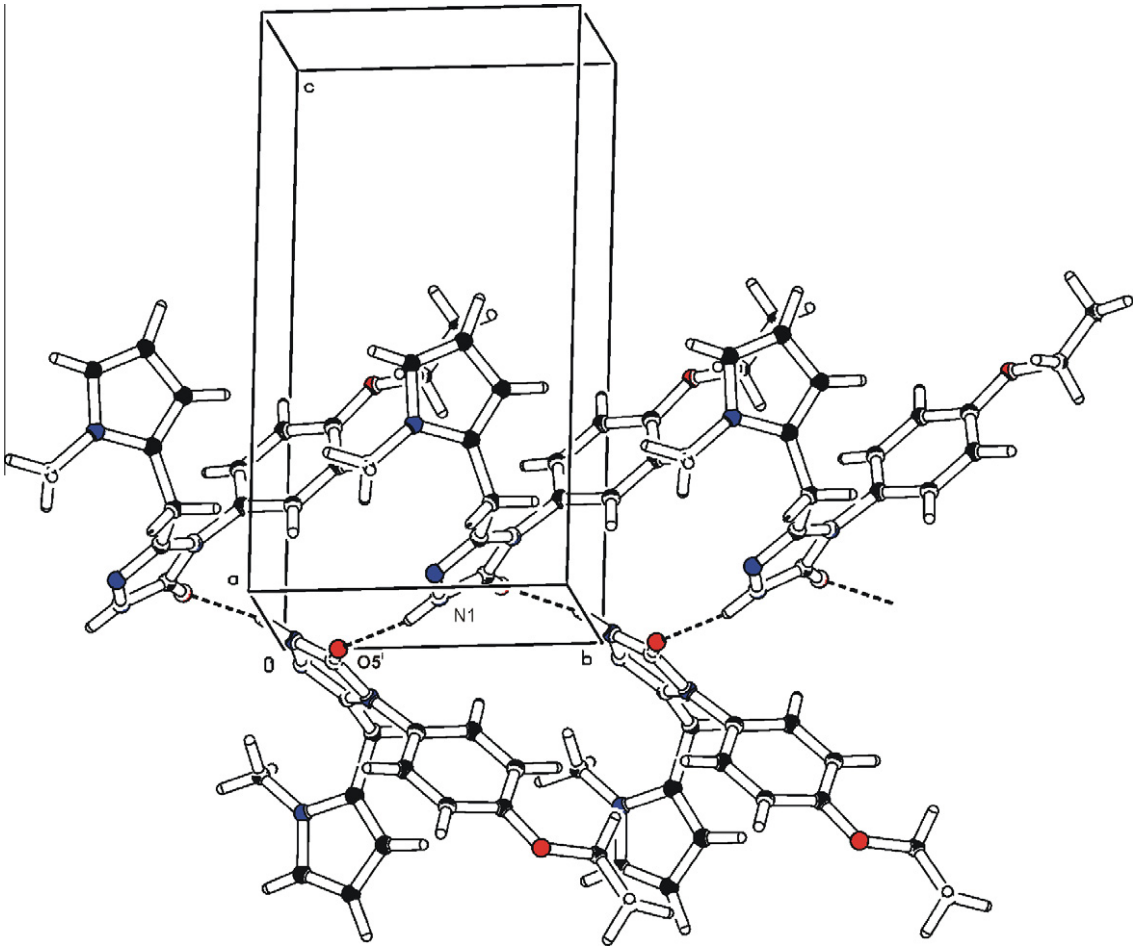

Fig. 3. The molecular packing of **1**, viewed down the a axis. Dashed lines indicate intermolecular hydrogen bonds (symmetry code: (i) =1 − *x*, −1/2 + *y*, −*z*).

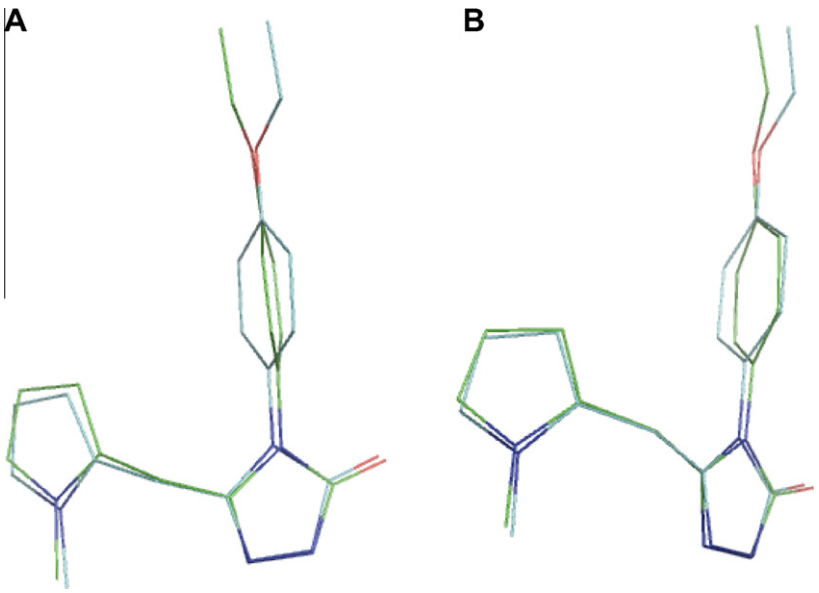

Fig. 4. The alignment of the X-ray and computed (A–HF, B– 3LYP DFT) structures of the investigated compound.

analysis and IR spectroscopy in KBr but do not confirm the shift of the tautomeric equilibrium towards the enol form in a chloroform solution.

The obtained results enrich the knowledge about structural chemistry of 1,2,4-triazol-5-ones and in this manner are important for basic research. It is worth stressing that only few studies have

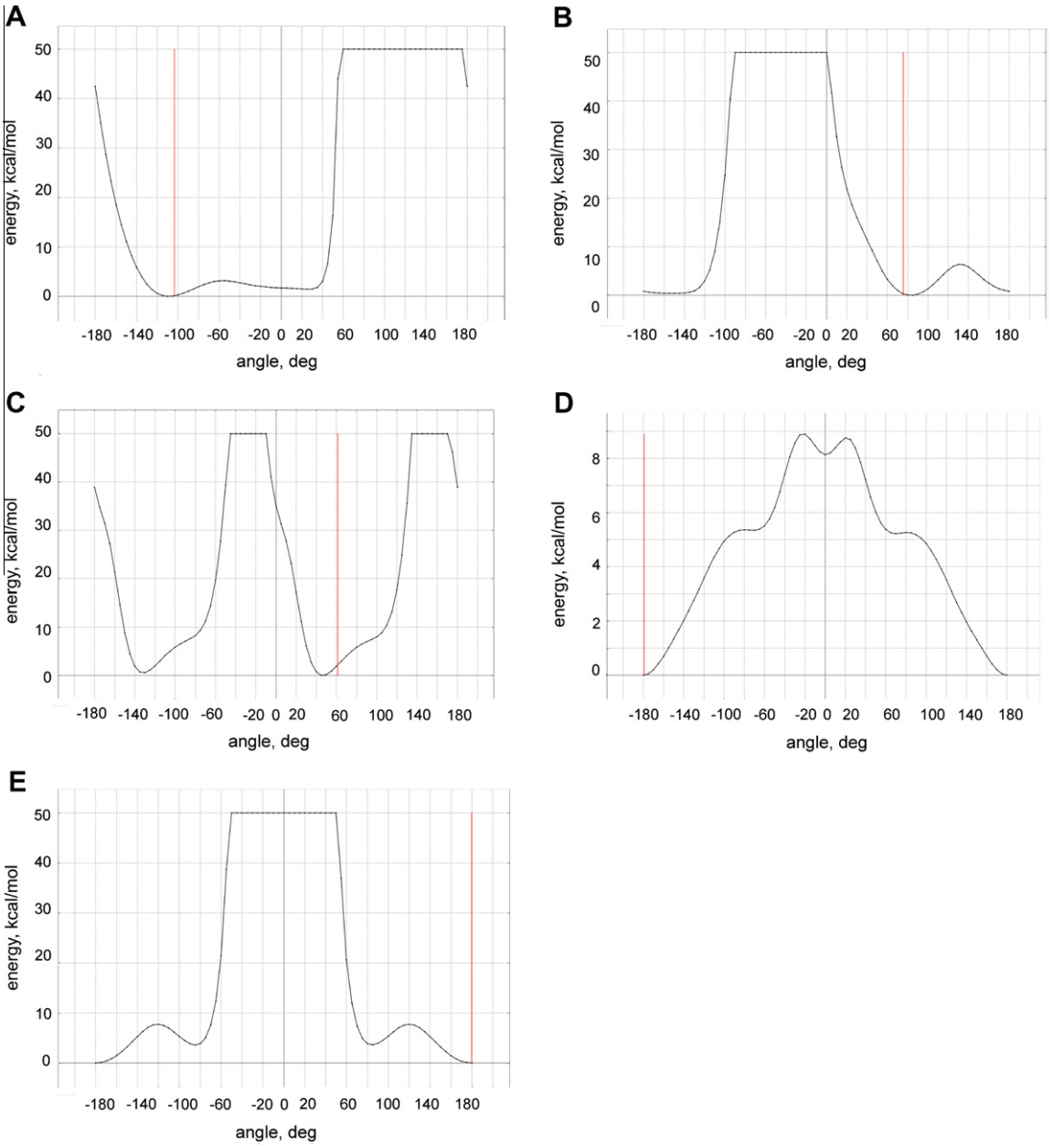

Fig. 5. Molecular energy profiles of the investigated compound against the selected degrees of torsional freedom: A—N2—C3—C6—C7; B—C3—C6—C7—N8; C—C5—N4—C21—C22; D—C23—C24—O27—C28 and E—C24—O27—C28—C29 The red line denotes the final conformer obtained with the B3LYP DFT method.

Table 5
The stabilization energy ΔE (kcal/mol) for the tautomeric forms of **1–6**.

Compound	Form	Gas phase		Chloroform		Water	
R		RHF/SCF ΔE	DFT ΔE	RHF/SCF ΔE	DFT ΔE	RHF/SCF ΔE	DFT ΔE
1	Ketone	0	0	0	0	0	0
	Enol	21.05	18.29	19.34	16.90	18.58	16.14
2	Ketone	0	0	0	0	0	0
	Enol	16.16	17.03	15.41	15.63	15.03	8.19
3	Ketone	0	0	0	0	0	0
	Enol	19.68	19.38	17.86	17.36	17.02	16.47
4	Ketone	0	0	0	0	0	0
	Enol	20.51	20.16	18.54	18.08	17.53	17.04
5	Ketone	0	0	0	0	0	0
	Enol	22.30	22.21	21.58	21.37	21.41	20.96
6	Ketone	0	0	0	0	0	0
	Enol	15.53	15.54	14.86	14.77	14.52	17.98

been reported for similar systems [29,40]. However, as it has been already mentioned, the significance of the obtained results on the keto–enol tautomerism of compounds **1–6** is mainly connected with their pharmacological activity. Determination that the keto form of **1–6** is a privileged one was a prerequisite for future SAR and molecular docking studies.

4. Conclusions

The results of experimental (X-ray, IR spectra) and computational studies indicate that, in the gas phase and in the crystalline state, all the investigated molecules exist in the keto form while in the chloroform solution a small amount of the enol form in the equilibrium with the keto form is observed. The results of the above studies are of crucial for chemistry of 1,2,4-triazol-5-ones as well as for future SAR and docking studies for this series of compounds.

Acknowledgments

This article was partially prepared during the postdoctoral fellowship of Agnieszka A. Kaczor, funded by the Foundation for Polish Science (FNP, Kulomb outgoing fellowship). Calculations with Gaussian03 were performed under a computational grant by Interdisciplinary Center for Mathematical and Computational Modeling (ICM), Warsaw, Poland, Grant No. G30-18. We thank Grzegorz Bakalarski, MSc, from the ICM for his help with Gaussian03 software. We also thank Prof. dr Hab. Zofia Rzączyńska from the Department of General and Coordination Chemistry of Maria Curie-Skłodowska University, Lublin, Poland for access to the GaussView software.

Appendix A. Supplementary material

Supplementary data associated with this article can be found, in the online version, at doi:10.1016/j.molstruc.2011.03.041.

References

[1] K. Zborowski, A. Korenova, M. Uher, M.L. Proniewicz, J. Mol. Struct. (Theochem) 683 (2004) 15.
[2] J. Nawrot-Modranka, E. Nawrot, J. Graczyk, Eur. J. Med. Chem. 41 (2006) 1301.
[3] D. Matosiuk, S. Fidecka, L. Antkiewicz-Michaluk, I. Dybała, A.E. Kozioł, Eur. J. Med. Chem. 36 (2001) 783.
[4] D. Matosiuk, S. Fidecka, L. Antkiewicz-Michaluk, J. Lipkowski, I. Dybala, A.E. Koziol, Eur. J. Med. Chem. 37 (2002) 761.
[5] D. Matosiuk, S. Fidecka, L. Antkiewicz-Michaluk, I. Dybala, A.E. Koziol, Eur. J. Med. Chem. 37 (2002) 845.
[6] K. Sztanke, S. Fidecka, E. Kedzierska, Z. Karczmarzyk, K. Pihlaja, D. Matosiuk, Eur. J. Med. Chem. 40 (2005) 127.
[7] C. Temperini, A. Cecchi, A. Scozzafava, C.T. Supuran, J. Med. Chem. 52 (2009) 322.
[8] H. Kumar, S.A. Javed, S.A. Khan, M. Amir, Eur. J. Med. Chem. 43 (2008) 2688.
[9] M. Moise, V. Sunel, L. Profire, M. Popa, J. Desbrieres, C. Peptu, Molecules 14 (2009) 2621.
[10] H. Bayrak, A. Demirbas, N. Demirbas, S.A. Karaoglu, Eur. J. Med. Chem. 44 (2009) 4362.
[11] M.A. Al-Omar, Molecules 15 (2010) 502.
[12] W.A. El-Sayed, O.M. Ali, S.R. El-Dakkony, A.A. Abdel-Rahman, Z. Naturforsch. 65c (2010) 15.
[13] R.C. Sanjeeva, R.L. Sanjeeva, K.G. Rajesh, A. Nagaraj, Chem. Pharm. Bull. 58 (2010) 1328.
[14] R.K. Singla, B.G. Varadaraj, J. Enzyme. Inhib. Med. Chem. 25 (2010) 696.
[15] E. Dogdas, B. Tozkoparan, F.B. Kaynak, L. Eriksson, E. Kuepeli, E.E. Yesilada, M. Ertan, Arzneim-Forsch. 57 (2007) 196.
[16] G. Aktay, B. Tozkoparan, M. Ertan, J. Enzyme Inhib. Med. Chem. 24 (2009) 898.
[17] B. Jiang, Y. Zeng, M.J. Li, J.Y. Xu, Y.N. Zhang, Q.J. Wang, N.Y. Sun, X.M. Wu, Arch. Pharm. 343 (2010) 500.
[18] V. Vivet-Boudou, J. Paillart, A. Burger, R. Marquet, Nucleosides, Nucleotides Nucleic Acids 26 (2007) 743.
[19] A. El-Essawy, W.A. El-Sayed, S.A. El-Kafrawy, A.S. Morshedy, A.H. Abdel-Rahman, Z. Naturforsch. 63c (2008) 667.
[20] R. Lesyk, O. Vladzimirska, S. Holota, L. Zaprutko, A. Gzella, Eur. J. Med. Chem. 42 (2007) 641.
[21] K. Sztanke, T. Tuzimski, J. Rzymowska, K. Pasternak, M. Kandefer-Szerszeń, Eur. J. Med. Chem. 43 (2008) 404.
[22] A. Pachuta-Stec, J. Rzymowska, L. Mazur, E. Mendyk, M. Pitucha, Z. Rzączyńska, Eur. J. Med. Chem. 44 (2009) 3788.
[23] M. Dobosz, M. Pitucha, I. Dybała, A.E. Kozioł, Collect. Czech. Chem. Commun. 68 (2003) 792.
[24] M. Dobosz, A. Maliszewska-Guz, M. Struga, Z. Kleinrok, E. Wielosz-Tokarzewska, E. Jagiełło-Wójtowicz, Acta Pol. Pharm. 58 (2001) 35.
[25] M. Wujec, M. Pitucha, M. Dobosz, Heterocycles 68 (2006) 779.
[26] M. Pitucha, B. Polak, R. Świeboda, U. Kosikowska, A. Malm, Z. Naturforsch. 64b (2009) 570.
[27] M. Pitucha, A. Chodkowska, R. Duda, E. Jagiełło-Wójtowicz, Z. Naturforsch. 64c (2009) 615.
[28] T.I. Vakulskaya, L.I. Larina, N.I. Protsuk, V.A. Lopyrev, Mag. Res. Chem. 47 (2009) 716.
[29] M.D. Davari, H. Bahrami, Z.Z. Haghighi, M. Zahedi, J. Mol. Model. 16 (2010) 841.
[30] N.R. Jadeja, R.N. Shirsat, E. Suresh, Struct. Chem. 16 (2005) 515.
[31] D. Ruiz, J. Giussi, A. Albesa, M. Schiavoni, J. Furlong, P. Allegretti, Spectrochim. Acta A Mol. Biomol. Spectrosc. 77 (2010) 485.
[32] V. Lacerda Jr., M.G. Constantino, G.V.J. da Silva, Á. Cunha Neto, C.F. Tormena, J. Mol. Struct. 828 (2007) 54.
[33] A.K. Samanta, P. Pandey, B. Bandyopadhyay, T. Chakraborty, J. Mol. Struct. 963 (2010) 234.
[34] H. Yüksek, O. Gürsoy, I. Cakmak, M. Alkan, Mag. Res. Chem. 43 (2005) 585.
[35] L. Xu, G. Fang, X. Li, J. Yuan, X. Hu, W. Zhu, H. Xiao, G. Ji, J. Mol. Graph. Model. 26 (2007) 415.
[36] H. Yüksek, M. Alkan, I. Cakmak, Z. Ocak, S. Bahçeci, M. Calapoğlu, M. Elmastas, A. Kolomuç, H. Aksu, Int. J. Mol. Sci. 9 (2008) 9, 12.
[37] H. Yüksek, M. Alkan, S. Bahçeci, I. Cakmak, Z. Ocak, H. Baykara, O. Aktas, E. Agyel, J. Mol. Struct. 873 (2008) 142.
[38] H. Ma, H. Xiao, J. Song, X. Ju, W. Zhu, K. Yu, Chem. Phys. 344 (2008) 79.
[39] M. Pitucha, P. Borowski, Z. Karczmarzyk, A. Fruziński, J. Mol. Struct. 919 (2009) 170.
[40] N. Süleymanoglu, R. Ustabas, Y. Bingöl Alpaslan, Y. Ünver, M. Turan, K. Sancak, J. Mol. Struct. 989 (2011) 101.
[41] A. Altomare, G. Cascarano, C. Giacovazzo, A. Guagliardi, J. Appl. Crystallogr. 26 (1993) 343.
[42] G.M. Sheldrick, SHELX97 (Includes SHELXS97, SHELXL97, CIFTAB), Programs for Crystal Structure Analysis (Release 97–2), University of Göttingen, Germany, 1997.
[43] G.M. Sheldrick, SADABS (Ver. 2.06), University of Göttingen, Germany, 2002.
[44] H.D. Flack, Acta Crystallogr. A39 (1983) 876.
[45] L.J. Farrugia, J. Appl. Crystallogr. 30 (1997) 565.
[46] M. Nardelli, Comput. Chem. 7 (1993) 95.
[47] A.L. Spek, J. Appl. Crystallogr. 36 (2003) 7.
[48] L.J. Farrugia, J. Appl. Crystallogr. 32 (1999) 837.
[49] A.D. Becke, J. Chem. Phys. 98 (1993) 5648.
[50] C. Lee, W. Yang, R.G. Parr, Phys. Rev., B 37 (1988) 785.
[51] M.J. Frisch, G.W. Trucks, H.B. Schlegel, G.E. Scuseria, M.A. Robb, J.R. Cheeseman, J.A. Montgomery, T. Vreven, K.N. Kudin, J.C. Burant, J.M. Millam, S.S. Iyengar, J. Tomasi, V. Barone, B. Mennucci, M. Cossi, G. Scalmani, N. Rega, G.A. Petersson, H. Nakatsuji, M. Hada, M. Ehara, K. Toyota, R. Fukuda, J. Hasegawa, M. Ishida, T. Nakajima, Y. Honda, O. Kitao, H. Nakai, M. Klene, X. Li, J.E. Knox, H.P. Hratchian, J.B. Cross, V. Bakken, C. Adamo, J. Jaramillo, R. Gomperts, R.E. Stratmann, O. Yazyev, A.J. Austin; R. Cammi, C. Pomelli, J.W. Ochterski, P.Y. Ayala, K. Morokuma, G.A. Voth, P. Salvador, J.J. Dannenberg, V.G. Zakrzewski, S. Dapprich, A.D. Daniels, M.C. Strain, O. Farkas, D.K. Malick, A.D. Rabuck, K. Raghavachari, J.B. Foresman, J.V. Ortiz, Q. Cui, A.G. Baboul, S. Clifford, J. Cioslowski, B.B. Stefanov, G. Liu, A. Liashenko, P. Piskorz, I. Komaromi, R.L. Martin, D.J. Fox, T. Keith, M.A. Al-Laham, C.Y. Peng, A. Nanayakkara, M. Challacombe, P.M.W. Gill, B. Johnson, W. Chen, M.W. Wong, C. Gonzalez, J.A. Pople, Gaussian 03 (Revision C.02) Gaussian, Inc., Wallingford CT, 2004.
[52] MOE Molecular Operating Environment 2009.10, Chemical Computing Group.
[53] S. Miertuš, J. Tomasi, Chem. Phys. 65 (1982) 239.
[54] R.I.I. Dennington, T. Keith, J. Millam, GaussView (Version 4.1.2.), Semichem Inc, Shawnee Mission, KS, 2007.
[55] A. Frisch, R.I.I. Dennington, T. Keith, J. Millam, A.B. Nielsen, A.J. Holder, J. Hiscocks, GaussView Reference (Version 4.0.) Gaussian Inc, Pittsburgh, 2007.
[56] A.P. Scott, L. Random, J. Phys. Chem. 100 (1996) 16502.
[57] Vibrational frequency scaling factors. <http://cccbdb.nist.gov/vsf.asp>.
[58] E.F. Pettersen, T.D. Goddard, C.C. Huang, G.S. Couch, D.M. Greenblatt, E.C. Meng, T.E. Ferrin, J. Comput. Chem. 25 (2004) 1605.
[59] C.F. Macrae, I.J. Bruno, J.A. Chisholm, P.R. Edgington, P. McCabe, E. Pidcock, L. Rodriguez-Monge, R. Taylor, J. van de Streek, P.A. Wood, J. Appl. Crystallogr. 41 (2008) 466.
[60] A. Pedretti, L. Villa, G. Vistoli, J. Comput. Aided Mol. Des. 18 (2004) 167.
[61] E. Krieger, G. Vriend, Bioinformatics 18 (2002) 315.
[62] The PyMOL Molecular Graphics System, Version 0.99, Schrödinger, LLC.
[63] N. Özdemir, M. Dinçer, A. Çukurovalı, O. Büyükgüngör, J. Mol. Model. 15 (2009) 1435.
[64] G. Rauhut, P. Pulay, J. Phys. Chem. 99 (1995) 3093.
[65] A.A. El-Azhary, A.A. Al-Kahtani, J. Phys. Chem. A 109 (2005) 4505.
[66] F.H. Allen, O. Kennard, D. G. Watson, L. Brammer, A.G. Orpen, R. Taylor, Typical interatomic distances: organic compounds, in: International Tables for Crystallography, Vol. C, Kluwer Academic Publishers, Dordrecht/Boston/London, 1995, pp. 685.
[67] C.H. Stam, H.C. van der Plas, Acta Crystallogr. B32 (1976) 1288.
[68] U. Corouh, B. Kahveci, S. Sasmaz, E. Agar, Y. Kim, A. Erdönmez, Acta Crystallogr. C59 (2003) o47.